Available online at www.sciencedirect.com
SCIENCE DIRECT
Catalysis Today 113 (2006) 230–234
CATALYSIS TODAY
www.elsevier.com/locate/cattod

Structural and optical properties of MoO_3 and V_2O_5 thin films prepared by Spray Pyrolysis

L. Boudaoud [a], N. Benramdane [a], R. Desfeux [b], B. Khelifa [c], C. Mathieu [c,*]

[a] *Laboratoire de Caractérisation et d'Élaboration de Caractérisation des Matériaux, Université Djilalli Liabes, BP 89, Sidi Bel Abbes 22000, Algérie*
[b] *Laboratoire de Physico-Chimie des Interfaces et des Applications, Université d'Artois, Lens, France*
[c] *Centre de Calcul et de Modélisaion de Lens, Université d'Artois, Faculté Jean Perrin, Rue Jean Souvraz, SP 18, 62307 Lens Cedex, France*

Available online 19 January 2006

Abstract

MoO_3 and V_2O_5 thin films were prepared on glass substrates by Spray Pyrolysis technique at a substrate temperature of 423 K. The precursor solutions were obtained by varying the concentrations of $MoCl_5$ and VCl_3 in bi-distilled water. The structural investigation conducted by X-ray diffraction showed that MoO_3 and V_2O_5 thin films were polycrystalline with orthorhombic structure. The optical properties studied in the 300–2500 nm range suggest that the thin film behaviours are related to bound electronic states. The optical band gaps have been estimated from slopes of $\ln(\alpha h\nu)$ versus $h\nu$ plots of MoO_3 and V_2O_5 films were 3.35 and 2.44 eV, respectively. The electrical conductivity was measured using four probes method.

Keywords: MoO_3; V_2O_5 thin films; Spray Pyrolysis; Structural properties; Optical properties; Conductivity

1. Introduction

V_2O_5 and MoO_3 are transition metal oxide semiconductors which received significant attraction due to their broad industrial applications especially in active electrode in rechargeable micro batteries [1]. Among the various transition metal oxides, V_2O_5 and MoO_3 are interesting materials for secondary Li battery because of their features such as high electro-chemical activity, high stability and high energy density [2,3]. They are also being used in optical switching, humidity sensors, and as electrochromic materials [4]. V_2O_5 can also be used in conjunction with molybdenum [5] and tungsten oxides [6] for charge balanced devices for display purposes in informatics, variable reflection mirrors, smart windows in energy efficient architecture, and selective H_2 sensor [7].

In this work, the synthesis of MoO_3 and V_2O_5 thin films by Spray Pyrolysis technique was investigated at 0.2 M concentration of spray solution and at glass substrate temperature equal to 423 K. We report the structural properties of MoO_3 and V_2O_5 thin films, the optical properties and the electrical conductivity.

2. Experimental procedure

MoO_3 and V_2O_5 thin films were obtained by Spray Pyrolysis technique. Molybdenum pentchloride and vanadium trichloride solutions with 0.2 M molar concentration have been used. The substrate temperature is equal to 423 K, compressed air of pressure 6 N cm^{-2} has been used as a carrier gas. The structural characterization has been carried out at room temperature in the θ–2θ scan mode using a Rigaku Miniflex diffractometer (Cu $K\alpha_1$ radiation, λ = 1.5406 Å). Optical measurements of the transmittance and reflectance were carried out in the wavelength (300–2500 nm) using a UV-visible-NIR JASCO type V-570 double beam spectrometer. The electrical conductivity of the thin films was measured by the four probe method.

3. Results and discussion

3.1. Structural properties

The sprayed films have different colours which varies form white for MoO_3 to pale yellow for V_2O_5. The XRD pattern for crystalline MoO_3 and V_2O_5 thin films are in Fig. 1(a) and (b), respectively. A good agreement between our data and those of MoO_3 powder file (JCPDS data number 75-0912 card)

* Corresponding author. Tel.: +33 321 791782; fax: +33 321 794782.
E-mail address: mathieu@univ-artois.fr (C. Mathieu).

0920-5861/$ – see front matter © 2005 Elsevier B.V. All rights reserved.
doi:10.1016/j.cattod.2005.11.072

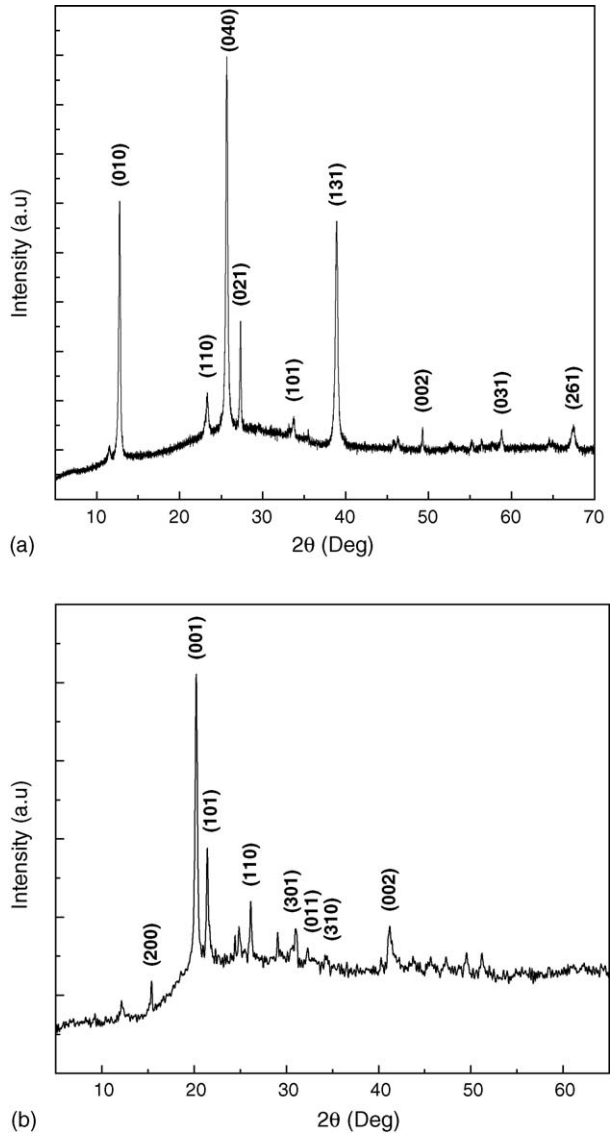

Fig. 1. (a) Experimental X-ray pattern of MoO_3 thin film. (b) Experimental X-ray pattern of V_2O_5 thin film.

corresponding to the MoO_3 with orthorhombic symmetry is obtained [10]. All peaks are indexed and the ($h\,k\,l$) peak existence indicates that the material crystallizes in a polycrystalline structure.

For the pattern in Fig. 1(b), there is a good agreement between the V_2O_5 inter-reticular distances and the JCPDS file (card no. 41-1426) corresponding to Pmmn spatial group of orthorhombic symmetry. The (0 0 l) peaks predominate indicating a preferential growth and the grains have the c-axis perpendicular to the substrate surface.

The lattice parameters have been calculated by using the following relation:

$$d_{hkl} = \frac{1}{\sqrt{(h^2/a^2) + (k^2/b^2) + (l^2/c^2)}} \quad (1)$$

with $a \neq b \neq c$ for orthorhombic lattice with ($h\,k\,l$) the Miller indices of reflector planes appearing on the XRD spectrum and $d_{h\,k\,l}$ their inter-reticular distances. Ours results are summarized in Table 1, these results are coherent with the published results [3,8,11,12].

Table 1
Lattice parameters of V_2O_5 and MoO_3 thin films

	Lattice parameters		
	a (Å)	b (Å)	c (Å)
V_2O_5			
Our result	11.51	3.56	4.38
[3]	11.50	3.56	4.34
[11]	11.51	3.56	4.37
MoO_3			
Our result	3.92	13.94	3.66
[12]	3.944	13.863	3.699
[8]	3.973	13.902	3.692

3.2. Optical measurements

3.2.1. Transmittance measurements

MoO_3 and V_2O_5 thin film optical properties were determined from the optical transmittance T and reflectance R, measured at room temperature with a non-polarized light. The measurements are recorded in the range 0.30–2.5 μm using a JASCO V-570 spectrophotometer. The transmittances T are shown in Fig. 2 for MoO_3 and V_2O_5 thin films respectively.

The spectra in Fig. 2 show a plate reaches 43% for V_2O_5 and 63% for MoO_3. The increase of the transmittance before the 500 nm is related to fundamental absorption, which permit to calculate the optical band gap.

3.2.2. Reflectivity spectra

Fig. 3 shows the reflectivity data for MoO_3 and V_2O_5. The spectra present two different behaviours. The reflectivity of MoO_3 is less than of V_2O_5. Instead, it exhibit a variable absorption and give a rise to absorption bands in the near infrared. Since the electrons in the thin film remain in bound or

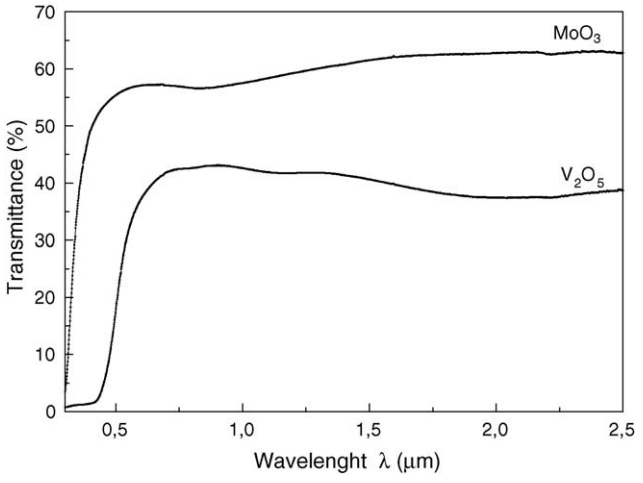

Fig. 2. Transmittance spectra for V_2O_5 and MoO_3 thin films.

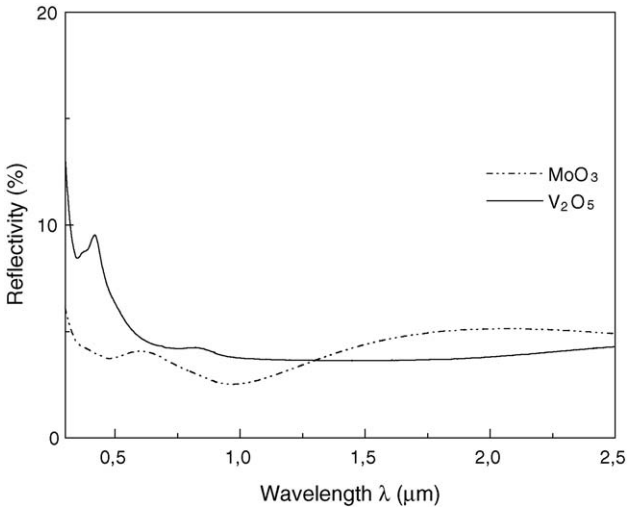

Fig. 3. Reflectivity spectra of V_2O_5 and MoO_3, thin films.

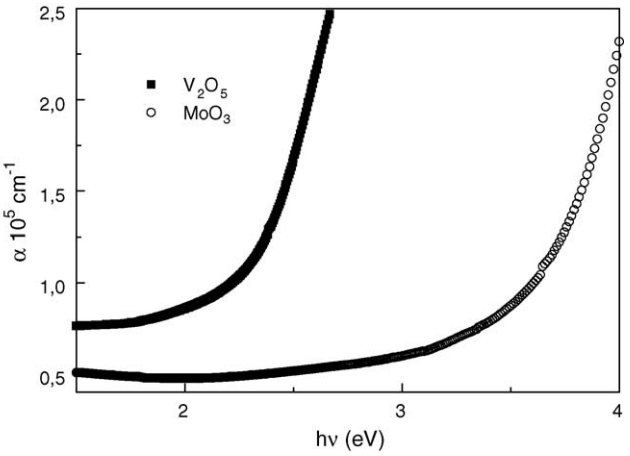

Fig. 4. Absorption coefficient of MoO_3 and V_2O_5 thin films.

highly localized states. For V_2O_5, a defined peak is observed in the spectrum which is related to the fundamental absorption.

The optical absorption increases with the increasing M^{4+}/M^{5+} ratio (M: metal), probably due to trapped electrons which are present at the M^{5+} sites. Moreover, the variable of absorption or broadening in the reflectivity minima has attributed to polaronic hopping process between V^{4+} and V^{5+} or between Mo^{5+} and Mo^{6+} sites [1–3,13].

3.2.3. Absorption coefficient

The α optical absorption coefficient was calculated from the following relation:

$$T = \frac{(1-R)^2\,\mathrm{e}^{-\alpha d}}{1-R^2\,\mathrm{e}^{-2\alpha d}} \tag{2}$$

where R and T are the spectral reflectance and transmittance and d is the film thickness. For thickness much greater than α^{-1}, the interference effects due to internal reflections as well as reflectance at normal incidence are negligible and the previous equation can be approximated by:

$$T \approx (1-R)^2 \exp(-\alpha d) \tag{3}$$

Optical coefficient α is given by the approximate formulae:

$$\alpha = \frac{1}{d_1 - d_2} \ln \frac{T_1}{T_2} \tag{4}$$

where T_1 and T_2 represent the transmission coefficients for two thin films prepared in the same conditions, d_1 and d_2 are their thicknesses.

The variations of the α absorption coefficient, as a function photon energy are presented in Fig. 4. The α values are in order of 105 cm^{-1}.

3.2.4. Determination of the gap energy

The fundamental absorption edge of semiconductors corresponds to the threshold for charge transitions between the highest nearly filled band and the lowest nearly empty band. The absorption is very small for photon energy much less than the energy gap and increases significantly for higher photon energies. The inter-band absorption theory shows that, the absorption coefficient near the threshold versus incident energy, is given by the following relation:

$$\alpha h\nu = A_n (h\nu - E_g)^{1/2} \tag{5}$$

where A_n is the probability parameter for the transition and E_g the optical gap energy. We have given the values of direct bands gaps transitions for V_2O_5 and for MoO_3 in Fig. 5(a) and (b) respectively. The linear region extrapolation gives the optical gaps energies of allowed direct transitions for spray pyrolysed MoO_3 and V_2O_5 polycrystalline thin films and are equal to 3.35 eV [9] and 2.44 eV [8] respectively.

In the indirect transitions where the electron is assisted by a single-phonon, the absorption coefficient can be described by:

$$\alpha h\nu = B_n (h\nu - E_{gi} \pm E_{ph})^2 \tag{6}$$

where E_{gi} is the gap due to the allowed indirect transitions, E_{ph} the phonon energy and B_n is a constant parameter. $+E_{ph}$ is the absorbed phonon energy and $-E_{ph}$ is the emitted phonon energy, during the transition process. The linear region extrapolation gives the indirect band gap energy for V_2O_5 thin film and it is shown in Fig. 5(c). The value of this gap is 1.737 eV [14].

3.2.5. Refractive index

In the higher energy region, an average value of the refractive index n for MoO_3 is 2.1, and for V_2O_5 is equal to 2.4. The n values are calculated by the relation:

$$n = \frac{1+R}{1-R} \pm \sqrt{\frac{4R}{(1-R)^2} - k^2} \tag{7}$$

where k is the extinction coefficient. This coefficient is deduced from the absorption coefficient by the classical relation $\alpha = 4\pi k/\lambda$, where λ is the wavelength of incident energy.

The variation of n versus λ are shown in Fig. 6 for MoO_3 and V_2O_5 thin films.

For MoO_3, the refractive index presents a minimum near 1 μm and a maximum near 1.8 μm. For V_2O_5, the spectrum

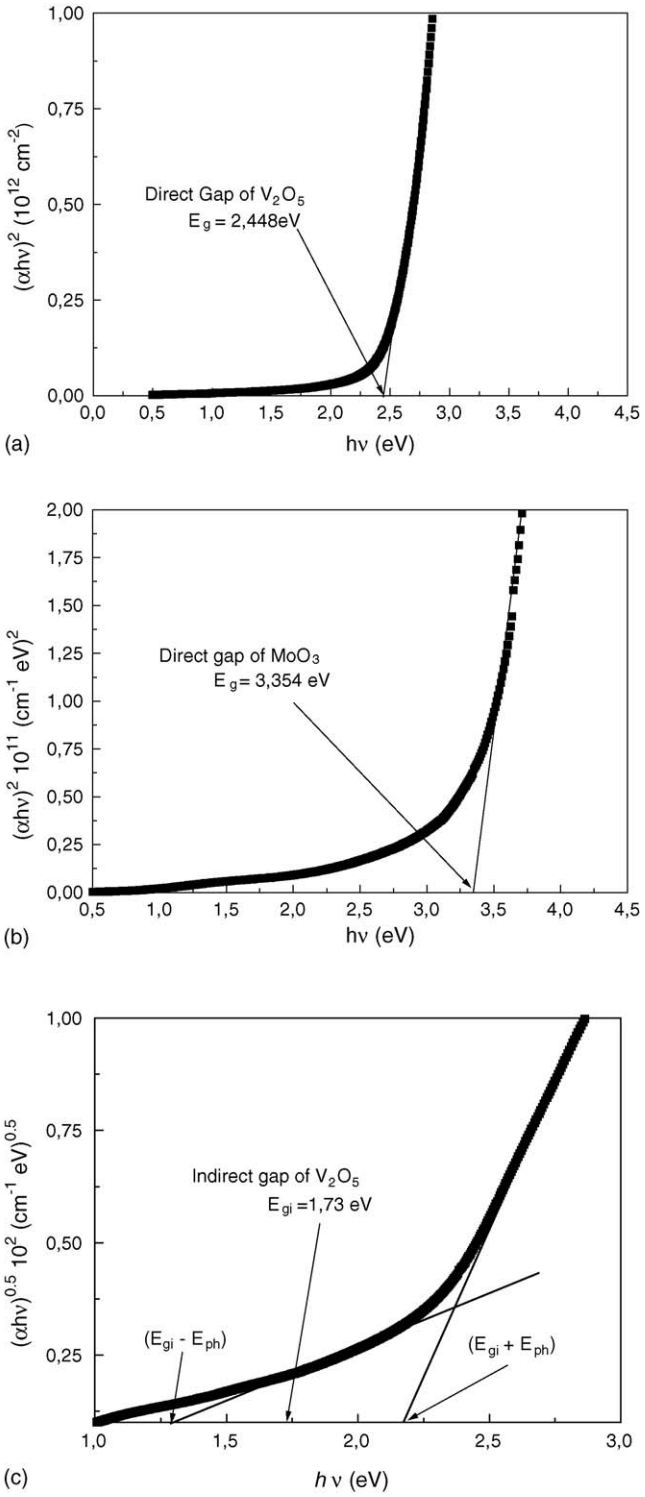

Fig. 5. (a) Plot of $(\alpha h\nu)^2$ vs. $h\nu$ for V_2O_5 thin film. (b) Plot of $(\alpha h\nu)^{0.5}$ vs. $h\nu$ for V_2O_5 thin film. (c) Plot of $(\alpha h\nu)^2$ vs. $h\nu$ for MoO_3 thin film.

shows a maximum before 0.5 μm and there is another small peak at 0.85 μm. These results seems to be characteristics of classical dispersion associated with bound electrons. The real part of the refractive index is low, compared with the values given for bulk. This low value can be attributed to the porous nature of the films [13]. The large effect of classical dispersion

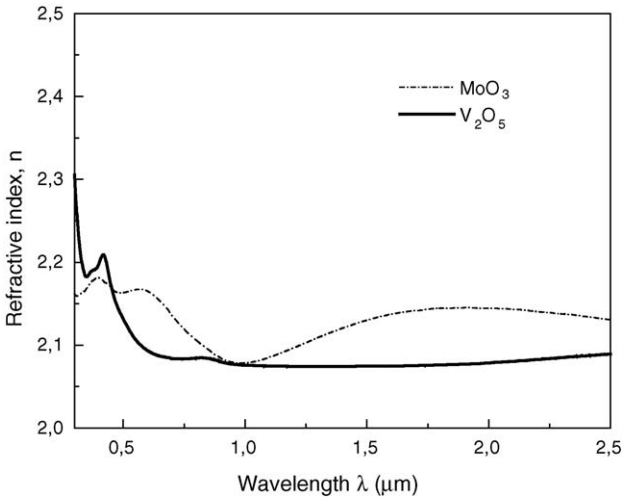

Fig. 6. Refractive index n for MoO_3 and V_2O_5 thin films.

of refractive index in the $n(\lambda)$ plots is pronounced in the short wavelength region. These are characteristics of no degenerate semiconductors, where bound electrons concentration is dominant. The high dispersion and high absorption especially around the fundamental absorption region can be described by the hopping process of small polaron from one levels set of localized states to a second set levels of localized states [3,13,15,16].

3.3. Electrical properties

Ambient temperature conductivity of the deposited thin films, prepared under the same conditions, was measured using a four probe method. The value of the conductivity for MoO_3 material was about $2.15 \times 10^{-6}\,\Omega^{-1}\,cm^{-1}$. The electrical conductivity increases until $1.09 \times 10^{-1}\,\Omega^{-1}\,cm^{-1}$ for V_2O_5.

4. Conclusion

MoO_3 and V_2O_5 thin films using Spray Pyrolysis method at substrate temperature of 423 K and for 0.2 M molar concentration have been obtained. The structural properties indicate polycrystalline structures for V_2O_5 and MoO_3. The reflectivity spectra of MoO_3 and V_2O_5 thin films were obtained for wavelength from 300 to 2500 nm. A detailed set of values of refractive index n were also determined from reflectivity data.

Reference

[1] K.V. Madhuri, B.S. Naidu, O.M. Hussain, Mater. Chem. Phys. 77 (2002) 22.
[2] C. Julien, G.A. Nazri, Solid State Batteries: Materials Design and Optimisation, Kluwer Academic Publishers, 1994.
[3] M. Balkanski, Solar Energy Mater. Solar Cells 62 (2000) 21.
[4] N. Özer, Thin Solid Films 305 (1997) 80.
[5] O. Mougin, J.L. Dubais, F. Mathieu, A. Rousset, J. Solid State Chem. 152 (2000) 353.
[6] N. Ozer, C.M. Lampert, Thin Solid Films 349 (1999) 205.

[7] C. Imawan, H. Steffes, F. Solzbacher, E. Obermeier, Technical University of Berlin, Microsensor and Actuator Technology (MAT), Sekr. TIB 3.1, Gustav-Meyer-Allee 25, Berlin, Germany.
[8] A. Bouzidi, N. Benramdane, A. Nakrela, C. Mathieu, B. Khelifa, R. Desfeux, Mater. Sci. Eng. B 95 (2002) 141.
[9] A. Bouzidi, N. Benramdane, H. Tabet-Derraz, C. Mathieu, B. Khelifa, R. Desfeux, Mater. Sci. Eng. B 97 (2003) 128.
[10] H.C. Zeng, J. Cryst. Growth 203 (1999) 547.
[11] C. Mathieu, S. Peralta, A. Da Costa, Y. Barbaux, Surf. Sci. 395 (1998) L201.
[12] W. Dong, A.N. Mansour, B. Dunn, Solid State Ionics 144 (2001) 31.
[13] Z. Hussain, J. Appl. Phys. 91 (9) (2002) 5745.
[14] V. Eyert, H. Höck, Phys. Rev. B, 57 20 (1998) 12727.
[15] M. Anwar, C.A. Hogarth, R. Bulpett, J. Matter. Sci. 24 (1989) 3087.
[16] N. Miyata, S. Akiyoshi, J. Appl. Phys. 58 (1985) 1651.